

PARAFAC-Based Unified Tensor Modeling for Wireless Communication Systems with Application to Blind Multiuser Equalization

André L. F. de Almeida ^{a,*} Gérard Favier ^{a,*} João Cesar M. Mota ^b

^a*Laboratoire I3S, CNRS/UNSA*

2000 Route des Lucioles, BP 121, 06903 Sophia Antipolis Cedex, France

Tel: +33 4 92 94 27 36; Fax: +33 4 92 94 28 96

^b*Wireless Telecom Research Group (GTEL), DETI/UFC*

Campus do Pici, CP 6005, 60455-970, Fortaleza, Ceará, Brazil

Abstract

In some antenna array based wireless communication systems the received signal is multidimensional and can be treated as a tensor (3D array) instead of a matrix (2D array). In this paper, we make use of a tensor decomposition known as PARAFAC (parallel factors) and propose a tensor (3D) model for the signal received by three types of wireless communication systems. The considered wireless communication systems are multiuser systems subject to frequency-selective multipath and employing multiple receiver antennas together with i) oversampling or ii) direct-sequence spreading or iii) multicarrier modulation. The proposed modeling approach aims at unifying the received signal model of these systems into a single PARAFAC model. We show that the proposed model has a constrained structure, where model constraints and associated dimensions depend on each particular system. The proposed PARAFAC model is demonstrated by expanding the tensor using Kronecker products of canonical vectors. As an application of this model to tensor signal processing, a new tensor-based receiver is proposed for blind multiuser equalization, which combines PARAFAC-based modeling with a subspace method. Simulation results are presented to illustrate the performance of the proposed blind receiver.

Key words: Alternating least squares, antenna arrays, blind equalization, direct-sequence spreading, frequency-selective multipath, multicarrier modulation, oversampling, parallel factor analysis, subspace, tensor modeling, wireless communications.

* Corresponding authors

Email addresses:

lima@i3s.unice.fr (André L. F. de Almeida), favier@i3s.unice.fr (Gérard

1 Introduction

Most of existing array signal processing approaches rely on matrix (2D arrays) models for the received signal. In wireless communication systems, array signal processing is generally used at the receiver to mitigate multiuser (co-channel) interference, inter-symbol interference as well as to benefit from spatial diversity available in the wireless channel. Usually considered signal processing dimensions are *space* and *time* dimensions. In space-time matrix models, space dimension usually varies along the rows of the received signal matrix while time dimension varies along the columns. However, the main limitation of working with a matrix model for the received signal is its lack of inherent uniqueness. Regarding the blind recovery of information, blind algorithms generally take special (problem-specific) structural properties of the transmitted signals into account such as orthogonality, finite-alphabet, constant-modulus or cyclostationarity in order to overcome the non-uniqueness of matrix decompositions and successfully perform multiuser signal separation and equalization [1–3].

Unlike 2D (matrix) models, the use of 3D (tensor) received signal models in array signal processing problems result from the incorporation of a third “axis”, also called dimension or mode, in addition to the usually considered *space* and *time* dimensions. For example, when temporal oversampling is used at the antenna array receiver, *oversampling* can be interpreted as the third dimension of the received signal. In a direct-sequence code division multiple access (DS/CDMA) system, *spreading* is the third dimension while in an orthogonal frequency division multiplexing (OFDM), *frequency* plays the role of this additional dimension. From a signal processing perspective, treating the received signal as a 3D tensor makes possible to simultaneously exploit the multiple forms of “diversity” inherent to it for a signal recovery purpose.

One of the most studied decompositions of 3D (or higher dimensional) tensors is called PARAFAC (parallel factor) analysis. PARAFAC was independently developed by Carroll and Chang [5] and Harshman [6] as a data analysis tool in psychometrics. It has also been widely studied in the context of chemometrics [7]. Several contributions bringing PARAFAC to the context of wireless communications have been carried out by Sidiropoulos and his co-workers (see [8] and the several references therein). In [9], the PARAFAC model has first appeared as a generalization of the ESPRIT method [10] for high-resolution direction finding. It has also been applied to the problem of multiuser detection for DS/CDMA systems in several works [11–14]. In [15], a PARAFAC receiver was also proposed for blind channel estimation in OFDM systems.

In this work, we present a new PARAFAC model for the received signal that is

Favier),

mota@gtel.ufc.br (João Cesar M. Mota)

valid for some multiuser wireless communication systems subject to frequency-selective multipath fading. The proposed model unifies the received signal model of three systems: i) a temporally-oversampled system, ii) a DS/CDMA system [16] and iii) an OFDM system [17]. For all these systems an antenna array is assumed at the receiver front-end. The proposed tensor model assumes specular multipath propagation, where each user in the system contributes with a finite number of multipaths to the received signal. We show that the proposed model is subject to structural constraints in some of its component matrices, and that the same “general” PARAFAC model is shared by the three considered systems. For each particular system, the model can be obtained from the general model by making appropriate choices in the structure/dimension of its matrix components. For the DS/CDMA system, our tensor modeling approach generalizes those of [12] and [13], which consider a special propagation model with a single path per user. It also covers the tensor model proposed in [18] as a special case, which assumes multiple paths per user but does not consider a frequency-selective channel model.

This paper is summarized as follows. In Section 2, the standard PARAFAC decomposition is briefly introduced. The proposed tensor decomposition is also described in this section. In Section 3, the general system model and assumptions are presented. In Section 4, the proposed tensor decomposition is used to model the received signal associated with temporally-oversampled, DS/CDMA and OFDM systems. Both scalar (multi-indexed) and matrix-slice notations are used to model the received signal in this section. In Section 5, we formalize the unified PARAFAC-based model for temporally-oversampled, DS/CDMA and OFDM systems. An application of the PARAFAC model to blind multiuser equalization is presented in Section 6, and a new blind receiver algorithm that combines PARAFAC-based modeling with a subspace method is proposed. In Section 7, simulation results are presented to illustrate the performance of this PARAFAC-based receiver for different propagation scenarios. Finally, Section 8 concludes this paper.

Notation and Properties: Some notations and properties are now recalled. \mathbf{A}^T , \mathbf{A}^{-1} and \mathbf{A}^\dagger stand for transpose, inverse and pseudo-inverse of \mathbf{A} , respectively. The operator $Diag(\mathbf{a})$ forms a diagonal matrix from its vector argument; $BlockDiag(\mathbf{A}_1 \cdots \mathbf{A}_N)$ constructs a block-diagonal matrix of N blocks from its argument matrices; $D_i(\mathbf{A})$ forms a diagonal matrix holding the i -th row of \mathbf{A} on its main diagonal; $vec(\cdot)$ stacks the columns of its matrix argument in a vector; \otimes and \diamond denote the Kronecker product and the Khatri-Rao product, respectively:

$$\mathbf{A} \diamond \mathbf{B} = [\mathbf{a}_1 \otimes \mathbf{b}_1, \dots, \mathbf{a}_R \otimes \mathbf{b}_R] \in \mathbb{C}^{IJ \times R},$$

where $\mathbf{A} = [\mathbf{a}_1 \dots \mathbf{a}_R] \in \mathbb{C}^{I \times R}$ and $\mathbf{B} = [\mathbf{b}_1 \dots \mathbf{b}_R] \in \mathbb{C}^{J \times R}$. Given $\mathbf{A} \in \mathbb{C}^{I \times R}$,

$\mathbf{B} \in \mathbb{C}^{J \times S}$, $\mathbf{C} \in \mathbb{C}^{R \times P}$ and $\mathbf{D} \in \mathbb{C}^{S \times P}$, we have:

$$(\mathbf{A} \otimes \mathbf{B})(\mathbf{C} \otimes \mathbf{D}) = \mathbf{AC} \otimes \mathbf{BD}. \quad (1)$$

2 Background on Parallel Factor (PARAFAC) decompositions

2.1 Standard PARAFAC decomposition

For an $I_1 \times I_2 \times I_3$ third-order tensor \mathcal{X} , its Q -component PARAFAC decomposition is given by:

$$x_{i_1, i_2, i_3} = \sum_{q=1}^Q a_{i_1}^{(q)} b_{i_2}^{(q)} c_{i_3}^{(q)}. \quad (2)$$

The standard PARAFAC model for a three-way (3D) array expresses the original tensor as a sum of rank-one three-way factors, each one of which being an outer product of three vectors. Figure (1) illustrates the PARAFAC decomposition of tensor \mathcal{X} . By analogy with the definition of matrix rank, the rank of a third-order tensor is defined as the minimum number of rank-one three-way components needed to decompose \mathcal{X} [4].

The PARAFAC decomposition can also be represented in matrix notation. Define an $I_1 \times Q$ matrix \mathbf{A} , $I_2 \times Q$ matrix \mathbf{B} and $I_3 \times Q$ matrix \mathbf{C} with respective elements $a_{i_1}^{(q)} = [\mathbf{A}]_{i_1, q}$, $b_{i_2}^{(q)} = [\mathbf{B}]_{i_2, q}$ and $c_{i_3}^{(q)} = [\mathbf{C}]_{i_3, q}$. Define also a set of $I_2 \times I_3$ matrices $\mathbf{X}_{i_1 \cdot \cdot}$, $i_1 = 1, \dots, I_1$, a set of $I_3 \times I_1$ matrices $\mathbf{X}_{\cdot i_2 \cdot}$, $i_2 = 1, \dots, I_2$ and a set of $I_1 \times I_2$ matrices $\mathbf{X}_{\cdot \cdot i_3}$, $i_3 = 1, \dots, I_3$. Based on these definitions, the model (2) can be written in three different ways:

$$\begin{aligned} \mathbf{X}_{i_1 \cdot \cdot} &= \sum_{q=1}^Q a_{i_1}^{(q)} \mathbf{b}^{(q)} \mathbf{c}^{(q)T} = \mathbf{B} D_{i_1}(\mathbf{A}) \mathbf{C}^T, \quad i_1 = 1, \dots, I_1, \\ \mathbf{X}_{\cdot i_2 \cdot} &= \sum_{q=1}^Q b_{i_2}^{(q)} \mathbf{c}^{(q)} \mathbf{a}^{(q)T} = \mathbf{C} D_{i_2}(\mathbf{B}) \mathbf{A}^T, \quad i_2 = 1, \dots, I_2, \\ \mathbf{X}_{\cdot \cdot i_3} &= \sum_{q=1}^Q c_{i_3}^{(q)} \mathbf{a}^{(q)} \mathbf{b}^{(q)T} = \mathbf{A} D_{i_3}(\mathbf{C}) \mathbf{B}^T, \quad i_3 = 1, \dots, I_3, \end{aligned}$$

where $\mathbf{a}^{(q)}$, $\mathbf{b}^{(q)}$ and $\mathbf{c}^{(q)}$ are the q -th column of matrices \mathbf{A} , \mathbf{B} and \mathbf{C} respectively, and the operator $D_{i_1}(\mathbf{A})$ forms a diagonal matrix with the i_1 -th row of \mathbf{A} . The matrices $\mathbf{X}_{i_1 \cdot \cdot}$, $i_1 = 1, \dots, I_1$, $\mathbf{X}_{\cdot i_2 \cdot}$, $i_2 = 1, \dots, I_2$, and $\mathbf{X}_{\cdot \cdot i_3}$, $i_3 = 1, \dots, I_3$ can be interpreted as slices of the tensor along the first, second and third dimensions, respectively. Stacking columnwise the matrix slices

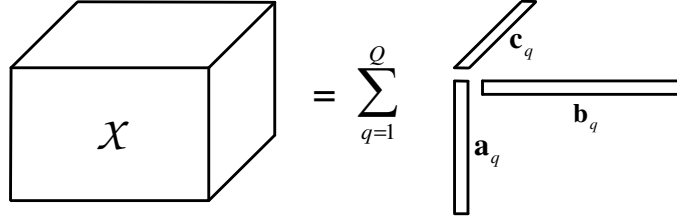


Fig. 1. Q -factor PARAFAC decomposition of a 3D tensor.

$\mathbf{X}_{..i_3}$, $i_3 = 1, \dots, I_3$ into a $I_3 I_1 \times I_2$ matrix, we get the unfolded matrix \mathbf{X}_1 :

$$\mathbf{X}_1 = \begin{bmatrix} \mathbf{X}_{..1} \\ \vdots \\ \mathbf{X}_{..I_3} \end{bmatrix} = \begin{bmatrix} \mathbf{A}D_1(\mathbf{C}) \\ \vdots \\ \mathbf{A}D_{i_3}(\mathbf{C}) \end{bmatrix} \mathbf{B}^T = (\mathbf{C} \diamond \mathbf{A})\mathbf{B}^T \quad (3)$$

Similarly, for the two other modes, we have:

$$\mathbf{X}_2 = \begin{bmatrix} \mathbf{X}_{1..} \\ \vdots \\ \mathbf{X}_{I_2..} \end{bmatrix} = \begin{bmatrix} \mathbf{C}D_1(\mathbf{B}) \\ \vdots \\ \mathbf{C}D_{I_2}(\mathbf{B}) \end{bmatrix} \mathbf{A}^T = (\mathbf{B} \diamond \mathbf{C})\mathbf{A}^T, \quad (4)$$

$$\mathbf{X}_3 = \begin{bmatrix} \mathbf{X}_{1..} \\ \vdots \\ \mathbf{X}_{I_1..} \end{bmatrix} = \begin{bmatrix} \mathbf{B}D_1(\mathbf{A}) \\ \vdots \\ \mathbf{B}D_{I_1}(\mathbf{A}) \end{bmatrix} \mathbf{C}^T = (\mathbf{A} \diamond \mathbf{B})\mathbf{C}^T, \quad (5)$$

where \mathbf{X}_2 and \mathbf{X}_3 are of dimensions $I_2 I_3 \times I_1$ and $I_1 I_2 \times I_3$ respectively. Uniqueness of the PARAFAC decomposition was firstly studied in [6,19], and more recently in [20,21]. The first formal proof was provided by Kruskal [4]. This proof has been recently revisited and clarified in [21]. In [22], the uniqueness condition was extended to the complex case while [23] further generalized this condition to tensors of an arbitrary order.

2.2 PAFAFAC-based decomposition with constrained structure

Let $\mathcal{X} \in \mathbb{C}^{I_1 \times I_2 \times I_3}$ be a third-order tensor and define two sets of matrices $\{\mathbf{A}^{(1)}, \dots, \mathbf{A}^{(Q)}\} \in \mathbb{C}^{I_1 \times R_1}$ and $\{\mathbf{B}^{(1)}, \dots, \mathbf{B}^{(Q)}\} \in \mathbb{C}^{I_2 \times R_2}$ with typical elements $a_{i_1, r_1}^{(q)} = [\mathbf{A}^{(q)}]_{i_1, r_1}$, $b_{i_2, r_2}^{(q)} = [\mathbf{B}^{(q)}]_{i_2, r_2}$, and a set of Q third-order tensors $\{\mathcal{C}^{(1)}, \dots, \mathcal{C}^{(Q)}\} \in \mathbb{C}^{R_1 \times R_2 \times I_3}$ with typical element $c_{r_1, r_2, i_3}^{(q)}$. The proposed de-

composition in scalar form is given by:

$$x_{i_1, i_2, i_3} = \sum_{q=1}^Q \sum_{r_1=1}^{R_1} \sum_{r_2=1}^{R_2} a_{i_1, r_1}^{(q)} b_{i_2, r_2}^{(q)} c_{r_1, r_2, i_3}^{(q)}. \quad (6)$$

This decomposition expresses the tensor x_{i_1, i_2, i_3} as a sum of Q trilinear blocks, each one of them being given by the sum of $R_1 R_2$ triple products. Define a set of Q matrices $\{\mathbf{C}^{(1)}, \dots, \mathbf{C}^{(Q)}\} \in \mathbb{C}^{I_3 \times R_1 R_2}$ in the following way:

$$[\mathbf{C}^{(q)}]_{i_3, (r_1-1)R_2+r_2} = c_{r_1, r_2, i_3}^{(q)}, \quad q = 1, \dots, Q,$$

where the matrix $\mathbf{C}^{(q)}$ is linked to tensor $\mathcal{C}^{(q)}$ by:

$$\mathbf{C}^{(q)} = [\text{vec}(\mathbf{C}_{\cdot 1}^{(q)T}) \cdots \text{vec}(\mathbf{C}_{\cdot I_3}^{(q)T})]^T,$$

$\mathbf{C}_{\cdot i_3}^{(q)} \in \mathbb{C}^{R_1 \times R_2}$ being the i_3 -th matrix slice of $\mathcal{C}^{(q)}$, $i_3 = 1, \dots, I_3$.

Let us define the block-matrices $\mathbf{A} = [\mathbf{A}^{(1)} \cdots \mathbf{A}^{(Q)}] \in \mathbb{C}^{I_1 \times Q R_1}$, $\mathbf{B} = [\mathbf{B}^{(1)} \cdots \mathbf{B}^{(Q)}] \in \mathbb{C}^{I_2 \times Q R_2}$ and $\mathbf{C} = [\mathbf{C}^{(1)} \cdots \mathbf{C}^{(Q)}] \in \mathbb{C}^{I_3 \times Q R_1 R_2}$, and block-diagonal constraint matrices $\bar{\Psi} = \mathbf{I}_Q \otimes (\mathbf{I}_{R_1} \otimes \mathbf{1}_{R_2}^T) = \mathbf{I}_Q \otimes \Psi$ and $\bar{\Phi} = \mathbf{I}_Q \otimes (\mathbf{1}_{R_1}^T \otimes \mathbf{I}_{R_2}) = \mathbf{I}_Q \otimes \Phi$, of dimensions $Q R_1 \times Q R_1 R_2$ and $Q R_2 \times Q R_1 R_2$ respectively. By analogy with (3), (4) and (5), the unfolded matrices \mathbf{X}_1 , \mathbf{X}_2 and \mathbf{X}_3 are given by:

$$\begin{aligned} \mathbf{X}_1 &= (\mathbf{C} \diamond \mathbf{A} \bar{\Psi}) \bar{\Phi}^T \mathbf{B}^T, \\ \mathbf{X}_2 &= (\mathbf{B} \bar{\Phi} \diamond \mathbf{C}) \bar{\Psi}^T \mathbf{A}^T, \\ \mathbf{X}_3 &= (\mathbf{A} \bar{\Psi} \diamond \mathbf{B} \bar{\Phi}) \mathbf{C}^T. \end{aligned} \quad (7)$$

The demonstration of (7) is provided in the Appendix, considering the unfolded matrix \mathbf{X}_3 . By comparing (7) with (3)-(5), we deduce the following correspondences: $\mathbf{A} \rightarrow \mathbf{A} \bar{\Psi}$, $\mathbf{B} \rightarrow \mathbf{B} \bar{\Phi}$ and $\mathbf{C} \rightarrow \mathbf{C}$. Therefore, $\mathbf{X}_{\cdot i_3} \in \mathbb{C}^{I_1 \times I_2}$ of \mathcal{X} can be expressed as:

$$\mathbf{X}_{\cdot i_3} = \sum_{q=1}^Q \mathbf{A}^{(q)} \Psi D_{i_3}(\mathbf{C}^{(q)}) (\mathbf{B}^{(q)} \Phi)^T. \quad (8)$$

A more compact notation for (8) is the following:

$$\mathbf{X}_{\cdot i_3} = \mathbf{A} \bar{\Psi} D_{i_3}(\mathbf{C}) (\mathbf{B} \bar{\Phi})^T. \quad (9)$$

An illustration of this decomposition is shown in Fig. 2.

Remark 1: Model (9) is a sort of rank-deficient PARAFAC model, which models interactions involving columns of the different component matrices. It is similar to the model proposed in [28], therein referenced as PARALIND

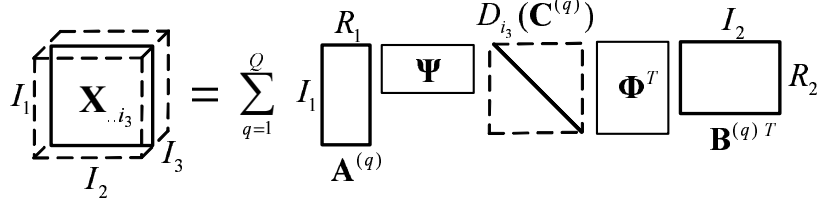


Fig. 2. Illustration of a PARAFAC decomposition with constrained structure.

(PARALLEL profiles with LINEAR Dependencies), although the modeling approach here is more general. The model proposed here, is a sort of “Block-PARAFAC” model composed of Q tensor blocks, where interactions involving factors of different modes are confined to each block. In [29] and [30], we propose a more general formulation of this model, considering that the interaction pattern may differ from block to block. In the context of this work, allowing different interaction patterns per block is equivalent to assume users with different number of multipaths as well as with different multipath structure [30].

2.2.1 Uniqueness

Consider the set of matrix-slices $\mathbf{X}_{..i_3}$, $i_3 = 1, \dots, I_3$, given in (8). Assume that the component matrices $\mathbf{A}^{(q)} \in \mathbb{C}^{I_1 \times R_1}$, $\mathbf{B}^{(q)} \in \mathbb{C}^{I_2 \times R_2}$ and $\mathbf{C}^{(q)} \in \mathbb{C}^{I_3 \times R_1 R_2}$ are full-column rank. If every set $\{\mathbf{A}^{(1)}, \dots, \mathbf{A}^{(Q)}\}$, $\{\mathbf{B}^{(1)}, \dots, \mathbf{B}^{(Q)}\}$ and $\{\mathbf{C}^{(1)}, \dots, \mathbf{C}^{(Q)}\}$ is linear independent, a necessary condition for the separation/resolution of the Q blocks is:

$$\min \left(\lfloor \frac{I_1 I_2}{R_1 R_2} \rfloor, \lfloor \frac{I_1 I_3}{R_2} \rfloor, \lfloor \frac{I_2 I_3}{R_1} \rfloor \right) \geq Q, \quad (10)$$

where $\lfloor \cdot \rfloor$ stands for the greatest integer number that is smaller than its argument. In this case, there are non-singular block-diagonal matrices $\mathbf{T}_a \in \mathbb{C}^{R_1 Q \times R_1 Q}$, $\mathbf{T}_b \in \mathbb{C}^{R_2 Q \times R_2 Q}$ and $\mathbf{T}_c \in \mathbb{C}^{R_1 R_2 Q \times R_1 R_2 Q}$, with diagonal blocks $\mathbf{T}_a^{(q)}$, $\mathbf{T}_b^{(q)}$ and $\mathbf{T}_c^{(q)}$ satisfying

$$(\mathbf{T}_a^{(q)} \otimes \mathbf{T}_b^{(q)})^{-1} = \mathbf{T}_c^{(q)T}, \quad q = 1, \dots, Q,$$

so that

$$\widehat{\mathbf{A}} = \mathbf{A}(\mathbf{\Pi} \otimes \mathbf{I}_{R_1})\mathbf{T}_a, \quad \widehat{\mathbf{B}} = \mathbf{B}(\mathbf{\Pi} \otimes \mathbf{I}_{R_2})\mathbf{T}_b, \quad \widehat{\mathbf{C}} = \mathbf{C}(\mathbf{\Pi} \otimes \mathbf{I}_{R_1 R_2})\mathbf{T}_c \quad (11)$$

give rise to the same $\mathbf{X}_{..i_3}$, $i_3 = 1, \dots, I_3$, where $\mathbf{\Pi} \in \mathbb{C}^{Q \times Q}$ is a block-permutation matrix. Permutation of the R_1 columns of $\mathbf{A}^{(q)}$, the R_2 columns of $\mathbf{B}^{(q)}$ and $R_1 R_2$ columns of $\mathbf{C}^{(q)}$, $q = 1, \dots, Q$, are considered unimportant and are ignored in (11).

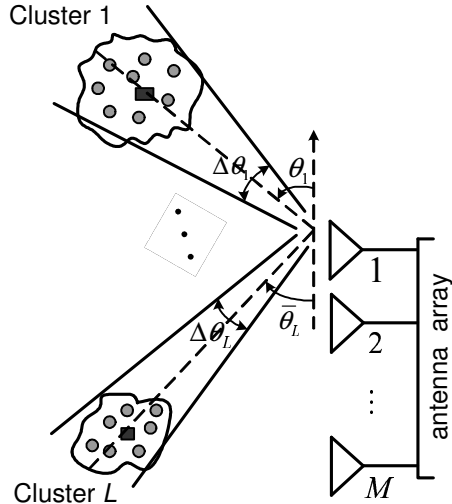


Fig. 3. Schematic representation of the multipath propagation scenario.

3 Channel and System Models

Let us consider a linear and uniformly-spaced array of M antennas receiving signals from Q co-channel users. Assume that the signal transmitted by each user is subject to multipath propagation and arrives at the receiver via L effective specular paths¹. The propagation channel is assumed to be time-dispersive and it is considered that multipath delay spread exceeds the inverse of the coherence bandwidth of the system, so that fading is frequency-selective. Following [24–26], we assume that there are L significant scatterer clusters (see Fig. 3) and that each of the multipaths emanating from the same scatterer cluster has the same delay. Each clustered multipath has a mean angle of arrival θ_l and an angle spread $\Delta\theta_l$. The adopted model is valid in practice, provided that the receive antenna array, generally located in a base transceiver station, is sufficiently high so that it is unobstructed and no local scattering occurs. These assumptions on the propagation scenario are typical for cellular suburban deployments [27], where the base transceiver station is on a tower or on the roof of a building.

The channel impulse response is assumed to span K symbols. The discrete-time base-band representation of the signal received at the m -th antenna of a linear and uniformly-spaced array at the n -th symbol interval is given by:

$$x_m(n) = \sum_{q=1}^Q \sum_{l=1}^L \beta_l^{(q)} a_m(\theta_{lq}) \sum_{k=1}^K g(k-1-\tau_{lq}) s^{(q)}(n-k+1) + v_m(n),$$

where $\beta_l^{(q)}$ is the fading envelope of the l -th path of the q -th user. The term

¹ In this model we have assumed that all users have the same number of multipaths in order to simplify the mathematical notation and the presentation of the model.

$a_m(\theta_{lq})$ is the response of the m -th antenna to the l -th path of the q -th user, θ_{lq} being the associated angle of arrival. Similarly, the term τ_{lq} is the propagation delay (normalized by the symbol period T) and the term $g(k-1-\tau_{lq})$ represents the k -th component of the pulse-shaping filter response. The channel impulse response has finite duration and is assumed to be zero outside the interval $[0, (K-1)T)$. Finally, $s^{(q)}(n)$ is the symbol transmitted by the q -th user at the n -th symbol interval and $v_m(n)$ is the measurement noise at the m -th antenna at the n -th symbol interval. The received signal vector $\mathbf{x}(n) \in \mathbb{C}^M$ is given by:

$$\mathbf{x}(n) = \sum_{q=1}^Q \sum_{l=1}^L \beta_l^{(q)} \mathbf{a}_l^{(q)} \mathbf{g}_l^{(q)T} \mathbf{s}^{(q)}(n) + \mathbf{v}(n),$$

where

$$\begin{aligned} \mathbf{a}_l^{(q)} &= [a_1(\theta_{lq}) \cdots a_M(\theta_{lq})]^T \in \mathbb{C}^M \\ \mathbf{g}_l^{(q)} &= [g(-\tau_{lq}) \cdots g(K-1-\tau_{lq})]^T \in \mathbb{R}^K \\ \mathbf{s}^{(q)}(n) &= [s^{(q)}(n) \cdots s^{(q)}(n-K+1)]^T \in \mathbb{C}^K, \end{aligned}$$

are the array steering vector, the pulse-shaping filter response vector and a symbol vector respectively, with $q = 1, \dots, Q$ and $l = 1, \dots, L$. For the q -th user, let us define:

$$\begin{aligned} \mathbf{A}^{(q)} &= [\mathbf{a}_1^{(q)} \cdots \mathbf{a}_L^{(q)}] \in \mathbb{C}^{M \times L} \\ \mathbf{b}^{(q)} &= [\beta_1^{(q)} \cdots \beta_L^{(q)}]^T \in \mathbb{C}^{L \times 1} \\ \mathbf{G}^{(q)} &= [\mathbf{g}_1^{(q)} \cdots \mathbf{g}_L^{(q)}]^T \in \mathbb{R}^{L \times K} \\ \mathbf{H}^{(q)} &= \text{Diag}(\mathbf{b}^{(q)}) \mathbf{G}^{(q)} \in \mathbb{C}^{L \times K} \\ \mathbf{S}^{(q)} &= [\mathbf{s}^{(q)}(1) \cdots \mathbf{s}^{(q)}(N)]^T \in \mathbb{C}^{N \times K}, \end{aligned}$$

where $\mathbf{A}^{(q)}$, $\mathbf{b}^{(q)}$ and $\mathbf{G}^{(q)}$ assemble L array responses, path gains and pulse shape responses respectively. $\mathbf{H}^{(q)}$ is the *overall* temporal channel response matrix associated with the q -th user, i.e. the pulse-shaping filter response matrix scaled by the multipath gains and $\mathbf{S}^{(q)}$ is Toeplitz, with the first row and column defined as $\mathbf{s}_{row}^{(q)} = [s^{(q)}(1) \ 0 \ \cdots \ 0]$ and $\mathbf{s}_{col}^{(q)} = [s^{(q)}(1) \ s^{(q)}(2) \ \cdots \ s^{(q)}(N)]^T$ respectively.

Assuming that the wireless channel is invariant during N consecutive symbol intervals, the received signal can be expressed as a matrix $\mathbf{X} \in \mathbb{C}^{M \times N}$ that can be decomposed in the following form:

$$\mathbf{X} = [\mathbf{x}(1) \cdots \mathbf{x}(N)] = \sum_{q=1}^Q \mathbf{A}^{(q)} \mathbf{H}^{(q)} \mathbf{S}^{(q)} + \mathbf{V}. \quad (12)$$

Now, defining:

$$\begin{aligned}\mathbf{A} &= [\mathbf{A}^{(1)} \dots \mathbf{A}^{(Q)}] \in \mathbb{C}^{M \times QL} \\ \mathbf{B} &= \text{Diag}([\mathbf{b}^{(1)T} \dots \mathbf{b}^{(Q)T}]) \in \mathbb{C}^{QL \times QL} \\ \mathbf{G} &= \text{BlockDiag}(\mathbf{G}^{(1)} \dots \mathbf{G}^{(Q)}) \in \mathbb{R}^{QL \times QK} \\ \mathbf{S} &= [\mathbf{S}^{(1)} \dots \mathbf{S}^{(Q)}] \in \mathbb{C}^{N \times QK},\end{aligned}$$

the received signal matrix (12) can be rewritten in a more compact block-matrix form as:

$$\mathbf{X} = \mathbf{AHS} + \mathbf{V}, \quad (13)$$

with $\mathbf{H} = \mathbf{BG} \in \mathbb{C}^{QL \times QK}$.

Model (13) serves as a reference model for the development of the new 3D PARAFAC-based model unifying the received signal model of temporally-oversampled, DS/CDMA and OFDM systems. In other words, the basic *space* and *time* dimensions of the received signal (13) that are represented by matrices \mathbf{A} and \mathbf{S} , will be similarly defined when considering the proposed tensor model, the main difference being in the incorporation of a third dimension to the received signal as a consequence of oversampling, spreading or multicarrier modulation.

4 Tensor Modeling of the Received Signal

The key step to obtain a 3D PARAFAC model is linked to an appropriate definition of the *overall* channel response matrix \mathbf{H} for each considered system. Thus, in the same way that \mathbf{A} and \mathbf{S} model the space and time dimensions of the 2D received signal model (13), \mathbf{H} models the third dimension for the proposed 3D tensor model. This additional dimension can be an *oversampling* dimension, a *spreading* dimension or a *frequency* dimension depending on the considered system. In the following, we define the concept of *overall channel response* for each one of the considered systems. Then, the tensor notation is introduced to model the received signal of each system as a 3D PARAFAC-based tensor model.

4.1 Temporally-Oversampled System

At the output of each receiver antenna, the signal is sampled at a rate that is P times the symbol rate. Due to temporal oversampling, the resolution of the pulse-shaping filter response is increased by a factor P , which also increases the temporal resolution of the received signal by the same factor. Such an increase

in the temporal resolution can be interpreted as an incorporation of a third axis (or dimension) to the received signal, called the *oversampling dimension*. We define the p -th oversample associated with the k -th component of the pulse-shaping filter response to the (l, q) -th path as the following third-order tensor:

$$g_{l,k,p}^{(q)} = g(k - 1 + (p - 1)/P - \tau_{lq}), \quad p = 1, \dots, P.$$

The overall channel response, array response and symbols are defined as:

$$h_{l,k,p}^{(q)} = \beta_l^{(q)} g_{l,k,p}^{(q)}, \quad a_{m,l}^{(q)} = a_m(\theta_{lq}), \quad s_{n,k}^{(q)} = s_q(n - k + 1).$$

The received signal can be interpreted as a 3D tensor $\mathcal{X} \in \mathbb{C}^{M \times N \times P}$. Its (m, n, p) -th scalar component can be decomposed as:

$$x_{m,n,p} = \sum_{q=1}^Q \sum_{l=1}^L a_{m,l}^{(q)} \sum_{k=1}^K h_{l,k,p}^{(q)} s_{n,k}^{(q)} + v_{m,n,p}. \quad (14)$$

By comparing with (6), we have the following correspondences:

$$(I_1, I_2, I_3, R_1, R_2, \mathbf{A}, \mathbf{B}, \mathbf{C}) \rightarrow (M, N, P, L, K, \mathbf{A}, \mathbf{S}, \mathbf{H}) \quad (15)$$

Equation (14) is the *scalar notation* for the received signal tensor. It expresses the received signal in the form of summations and products involving three factors $a_{m,l}^{(q)}$, $h_{l,k,p}^{(q)}$ and $s_{n,k}^{(q)}$ associated with space, oversampling and time dimensions of the received signal, respectively. (14) can be alternatively written in matrix-slice form. Let us define a pulse-shape response matrix $\mathbf{G}_l^{(q)} \in \mathbb{R}^{P \times K}$ as:

$$\mathbf{G}_l^{(q)} = [\mathbf{g}_{l,1}^{(q)} \ \mathbf{g}_{l,2}^{(q)} \ \dots \ \mathbf{g}_{l,K}^{(q)}],$$

where $\mathbf{g}_{l,k}^{(q)} = [g_{l,k,1}^{(q)} \ g_{l,k,2}^{(q)} \ \dots \ g_{l,k,p}^{(q)}]^T \in \mathbb{R}^P$ collects the P oversamples associated with the k -th component of the (l, q) -th pulse-shape response. Define also $\mathbf{G}^{(q)} = [\mathbf{G}_1^{(q)} \ \dots \ \mathbf{G}_L^{(q)}] \in \mathbb{R}^{P \times LK}$ as a matrix concatenating the L pulse-shape response vectors associated with the q -th user. The overall temporal channel response matrix $\mathbf{H}^{(q)}$ can be expressed as:

$$\mathbf{H}^{(q)} = \mathbf{G}^{(q)} (\text{Diag}(\mathbf{b}^{(q)}) \otimes \mathbf{I}_K) \in \mathbb{C}^{P \times LK}. \quad (16)$$

Fixing the oversampling dimension, and using the analogy with (8) and the correspondences (15), the space-time slice $\mathbf{X}_{..p} \in \mathbb{C}^{M \times N}$, $p = 1, \dots, P$, can be factored as:

$$\mathbf{X}_{..p} = \sum_{q=1}^Q \mathbf{A}^{(q)} \mathbf{\Psi} D_p(\mathbf{H}^{(q)}) (\mathbf{S}^{(q)} \mathbf{\Phi})^T + \mathbf{V}_{..p}, \quad p = 1, \dots, P, \quad (17)$$

where $\mathbf{\Psi} = \mathbf{I}_L \otimes \mathbf{1}_K^T$ and $\mathbf{\Phi} = \mathbf{1}_L^T \otimes \mathbf{I}_K$ are the constraint matrices of the tensor model.

4.2 DS/CDMA System

At the transmitter, each symbol is spread by a signature (spreading code) sequence of length J with period $T_c = T/J$, where T is the symbol period. The spreading sequence associated with the q -th user is denoted by $\mathbf{c}^{(q)} = [c_1^{(q)} c_2^{(q)} \dots c_J^{(q)}]^T \in \mathbb{C}^J$. As a result of spreading operation, each symbol to be transmitted is converted into J chips. The chip-sampled pulse-shape response to the (l, q) -th path is defined in scalar form as:

$$g_{l,k,j}^{(q)} = g(k - 1 + (j - 1)/J - \tau_{lq}), \quad j = 1, \dots, J.$$

A scalar component of the overall channel response, i.e. including path gains, is defined as $h_{l,k,j}^{(q)} = \beta_l^{(q)} g_{l,k,j}^{(q)}$. The received signal can be interpreted as a 3D tensor $\mathcal{X} \in \mathbb{C}^{M \times N \times J}$ and its (m, n, j) -th scalar component has the following factorization:

$$x_{m,n,j} = \sum_{q=1}^Q \sum_{l=1}^L a_{m,l}^{(q)} \sum_{k=1}^K \sum_{j'=1}^J h_{l,k,j-j'}^{(q)} c_{j'}^{(q)} s_{n,k}^{(q)} + v_{m,n,j}. \quad (18)$$

Equation (18) decomposes the received signal in the form of summations and products involving four scalar factors $a_{m,l}^{(q)}$, $h_{l,k,j}^{(q)}$, $c_j^{(q)}$ and $s_{n,k}^{(q)}$. Defining

$$u_{l,k,j}^{(q)} = \sum_{j'=1}^J h_{l,k,j-j'}^{(q)} c_{j'}^{(q)}$$

as the convolution between the spreading sequence and the overall channel response, we can rewrite (18) as:

$$x_{m,n,j} = \sum_{q=1}^Q \sum_{l=1}^L a_{m,l}^{(q)} \sum_{k=1}^K u_{l,k,j}^{(q)} s_{n,k}^{(q)} + v_{m,n,j}. \quad (19)$$

Note that (19) is equivalent to (14), where $u_{l,k,j}^{(q)}$ plays the role of $h_{l,k,p}^{(q)}$ and $J \rightarrow P$. Therefore, by fixing the spreading dimension and slicing the received signal tensor $\mathcal{X} \in \mathbb{C}^{M \times N \times J}$ along the third-dimension, its j -th slice $\mathbf{X}_{..j} \in \mathbb{C}^{M \times N}$, $j = 1, \dots, J$, is given by:

$$\mathbf{X}_{..j} = \sum_{q=1}^Q \mathbf{A}^{(q)} \mathbf{\Psi} D_j(\mathbf{U}^{(q)}) (\mathbf{S}^{(q)} \mathbf{\Phi})^T + \mathbf{V}_{..j}, \quad j = 1, \dots, J, \quad (20)$$

where $\mathbf{U}^{(q)}$ is defined as:

$$\mathbf{U}^{(q)} = \mathbf{C}^{(q)} \mathbf{H}^{(q)} \in \mathbb{C}^{J \times KL}, \quad (21)$$

$\mathbf{C}^{(q)} \in \mathbb{C}^{J \times J}$ being a Toeplitz matrix with first row and column defined as $\mathbf{c}_{row}^{(q)} = [c^{(q)}(1) 0 \cdots 0]$ and $\mathbf{c}_{col}^{(q)} = [c^{(q)}(1) c^{(q)}(2) \cdots c^{(q)}(J)]^T$ respectively, and $\mathbf{H}^{(q)}$ being analogous to that defined in (16), where J replaces P .

4.3 OFDM System

In an OFDM system, the symbol sequence to be transmitted is organized into blocks of F symbols (serial-to-parallel conversion). Multicarrier modulation consists in linearly combining the F symbols using an inverse $N \times N$ Fast Fourier Transform (IFFT) matrix. After the IFFT stage, a cyclic prefix (CP) of length K is inserted to each OFDM block², before transmission. Due to the insertion of CP, the resulting OFDM block has length $F + K$. At the receiver inverse processing is done. The CP is removed and each received OFDM block is linearly combined using an $N \times N$ Fast Fourier Transform (FFT) matrix. Thanks to the use of IFFT/FFT together with insertion/removal of the CP, it can be shown [17] that the length- K convolutive channel is converted into a set of F scalar channels, i.e. the overall channel at each subcarrier is frequency-flat. This means that the overall channel matrix has a diagonal frequency response.

Let us define $h_{l,f}^{(q)} = \beta_l^{(q)} g_{l,f}^{(q)}$ as a scalar component of the overall frequency channel response at the f -th subcarrier, associated with the (l, q) -th path. The scalar $s_{n,f}^{(q)}$ denotes the f -th symbol of the n -th OFDM block associated with the q -th user. The received signal is also a 3D tensor and its (m, n, f) -th scalar component can be decomposed as:

$$x_{m,n,f} = \sum_{q=1}^Q \sum_{l=1}^L a_{m,l}^{(q)} h_{l,f}^{(q)} s_{n,f}^{(q)} + v_{m,n,f}. \quad (22)$$

As it has been done for the previous systems, we are interested in representing the received signal tensor in matrix- slice notation. Let us define the vector $\mathbf{s}_n^{(q)} = [s_{1,n}^{(q)} s_{2,n}^{(q)} \cdots s_{F,n}^{(q)}]^T \in \mathbb{C}^F$ collecting the symbols associated with the n -th OFDM block, $n = 1, \dots, N$. We define $\check{\mathbf{G}}_l^{(q)} \in \mathbb{R}^{F \times F}$ as a *circulant channel matrix* built up from the (l, q) -th pulse-shape response $\mathbf{g}_l^{(q)} = [g_{l,1}^{(q)} g_{l,2}^{(q)} \cdots g_{l,K}^{(q)}]^T \in \mathbb{R}^K$. Let

$$\Omega_{cp} = \begin{bmatrix} \mathbf{0}_{K \times (F-K)} & \mathbf{I}_K \\ & \mathbf{I}_F \end{bmatrix}, \quad \bar{\Omega}_{cp} = [\mathbf{0}_{F \times K} \quad \mathbf{I}_F],$$

be the matrices that represent the insertion and removal of the CP, of dimensions $(F + K) \times F$ and $F \times (F + K)$ respectively, and define a $(F + K) \times (F + K)$

² The CP is used to avoid interference between adjacent OFDM blocks. Its length should exceed the maximum delay spread of the channel. See [17] for further details.

Toeplitz matrix $\tilde{\mathbf{G}}_l^{(q)} = \text{Toeplitz}[\mathbf{g}_l^{(q)}]$. The (l, q) -th circulant matrix $\check{\mathbf{G}}_l^{(q)}$ is given by:

$$\check{\mathbf{G}}_l^{(q)} = \bar{\Omega}_{cp} \tilde{\mathbf{G}}_l^{(q)} \Omega_{cp}.$$

Note that the circulant structure of $\check{\mathbf{G}}_l^{(q)} \in \mathbb{C}^{F \times F}$ is an equivalent representation of the convolution matrix $\tilde{\mathbf{G}}_l^{(q)}$, when it is pre- and post-multiplied by the matrices that represent the removal and insertion of the CP, respectively. For further details on this construction, please see [17].

Define $\check{\mathbf{G}}^{(q)} = [\check{\mathbf{G}}_1^{(q)} \dots \check{\mathbf{G}}_L^{(q)}] \in \mathbb{R}^{F \times LF}$ as a *block-circulant* matrix concatenating the L circulant channel matrices associated with the q -th user. By analogy with (16), the *overall circulant channel matrix* $\check{\mathbf{H}}^{(q)}$ can be written as:

$$\check{\mathbf{H}}^{(q)} = \check{\mathbf{G}}^{(q)} \left(\text{Diag}(\mathbf{b}^{(q)}) \otimes \mathbf{I}_F \right) \in \mathbb{C}^{F \times LF}.$$

Taking IFFT/FFT transformations at the transmitter/receiver into account, the q -th user *overall frequency response channel matrix* $\mathbf{\Lambda}^{(q)} = [\mathbf{\Lambda}_1^{(q)} \dots \mathbf{\Lambda}_L^{(q)}] \in \mathbb{C}^{F \times LF}$, can be expressed as:

$$\mathbf{\Lambda}^{(q)} = \mathbf{\Gamma} \check{\mathbf{H}}^{(q)} (\mathbf{I}_L \otimes \mathbf{\Gamma})^H, \quad (23)$$

where $\mathbf{\Gamma} \in \mathbb{C}^{F \times F}$ is a FFT matrix the (i, k) -th entry of which is given by $\gamma_{i,k} = (1/\sqrt{F}) \cdot \exp(-j2\pi ik/N)$, $i, k = 0, 1, \dots, N-1$. Note that $\mathbf{\Lambda}_l^{(q)}$ is a diagonal matrix holding the vector $\mathbf{h}_l^{(q)} = [h_{1,l}^{(q)} h_{2,l}^{(q)} \dots h_{F,l}^{(q)}]^T$, on its diagonal, $l = 1, \dots, L$, i.e., $\mathbf{\Lambda}_l^{(q)} = \text{Diag}(\mathbf{h}_l^{(q)})$.

Now, collect N symbol blocks in $\mathbf{S}^{(q)} = [\mathbf{s}_1^{(q)} \dots \mathbf{s}_N^{(q)}] \in \mathbb{C}^{F \times N}$. Taking these definitions into account, the f -th slice $\mathbf{X}_{..f} \in \mathbb{C}^{M \times N}$, $f = 1, \dots, F$, of the received signal tensor $\mathcal{X} \in \mathbb{C}^{M \times N \times F}$ can be decomposed as:

$$\mathbf{X}_{..f} = \sum_{q=1}^Q \mathbf{A}^{(q)} \mathbf{\Psi} D_f(\mathbf{\Lambda}^{(q)}) (\mathbf{S}^{(q)} \mathbf{\Phi})^T + \mathbf{V}_{..f}, \quad f = 1, \dots, F. \quad (24)$$

Remark 2: It is worth noting that (17), (20) and (24) are similar PARAFAC-based decompositions, and all of them follow (8). The main differences are in the structure and/or in dimension of certain component matrices, but the general tensor formulation is identical. Such similarity is our main motivation to formalize a “general” or *unified* PARAFAC-based tensor model. This is done in the following section.

5 Unified PARAFAC model

In this section we formalize the unified PARAFAC model for the temporally-oversampled, DS/CDMA and OFDM systems. The proposed PARAFAC model brings together the tensor modeling of the received signal for these systems in a single model using a unified mathematical notation. The proposal of a unique model is based on the observation that the received signal for the three considered systems can be formulated as 3D tensors following fundamentally the same PARAFAC decomposition.

For convenience, we rewrite the scalar representations for the received signal given by (14), (19) and (22) for the temporally-oversampled, DS/CDMA and OFDM systems respectively, in the following way:

$$\begin{aligned}
 x_{m,n,p} &= \sum_{q=1}^Q \sum_{l=1}^L \sum_{k=1}^K a_{m,l}^{(q)} s_{n,k}^{(q)} h_{l,k,p}^{(q)} + v_{m,n,p}, \\
 x_{m,n,j} &= \sum_{q=1}^Q \sum_{l=1}^L \sum_{k=1}^K a_{m,l}^{(q)} s_{n,k}^{(q)} u_{l,k,j}^{(q)} + v_{m,n,j}, \quad u_{l,k,p}^{(q)} = h_{l,k,j}^{(q)} * c_j^{(q)}, \\
 x_{m,n,f} &= \sum_{q=1}^Q \sum_{l=1}^L \sum_{f'=1}^F a_{m,l}^{(q)} s_{n,f'}^{(q)} h_{l,f',f}^{(q)} + v_{m,n,f}, \quad h_{l,f',f}^{(q)} = h_{l,f}^{(q)} \delta_{f'f}.
 \end{aligned} \tag{25}$$

The three tensor models are quite similar. Note that the basic difference is on the definition of the term associated with the third-dimension of the equivalent PARAFAC model, which is $h_{l,k,p}^{(q)}$ for oversampled case, $u_{l,k,j}^{(q)}$ for the DS/CDMA case and $h_{l,f',f}^{(q)}$ for the OFDM case. Another difference is on the structure of the component matrix $\mathbf{S}^{(q)}$, which is not Toeplitz in the OFDM model.

In order to link the unified tensor model to (6), we define I_3 as the length of the third dimension of the received signal tensor. For the temporally-oversampled system $(I_3, R_2) = (P, K)$, for the DS/CDMA system $(I_3, R_2) = (J, K)$ and for the OFDM system $(I_3, R_2) = (F, F)$. The other parameters, which are common for all the systems are $I_1 = M$, $I_2 = N$, $R_1 = L$. In its general form, the tensor modeling of the three systems can be unified in the following expression:

$$\mathbf{X}_{..i_3} = \sum_{q=1}^Q \mathbf{A}^{(q)} \mathbf{\Psi} D_{i_3}(\mathbf{W}^{(q)}) (\mathbf{S}^{(q)} \mathbf{\Phi})^T + \mathbf{V}_{..i_3}, \quad i_3 = 1, \dots, I_3,$$

where

$$\mathbf{\Psi} = \mathbf{I}_L \otimes \mathbf{1}_{R_2}^T \in \mathbb{C}^{L \times LR_2}, \quad \mathbf{\Phi} = \mathbf{1}_L^T \otimes \mathbf{I}_{R_2} \in \mathbb{C}^{LR_2 \times R_2},$$

and $\mathbf{W}^{(q)}$ is either $\mathbf{H}^{(q)}$ (c.f. (16)), or $\mathbf{U}^{(q)}$ (c.f. (21)) or $\mathbf{\Lambda}^{(q)}$ (c.f. (23)), depending on the considered system.

Finally, concatenating I_3 space-time slices $\mathbf{X}_{..i_3}$, $i_3 = 1, \dots, I_3$ and using (7), we get:

$$\mathbf{X}_1 = (\mathbf{W} \diamond \mathbf{A} \bar{\Psi})(\mathbf{S} \bar{\Phi})^T, \quad (26)$$

where $\bar{\Psi} = \mathbf{I}_Q \otimes \Psi$ and $\bar{\Phi} = \mathbf{I}_Q \otimes \Phi$. The factorization of $\mathbf{X}_2 = [\mathbf{X}_{.1}^T \dots \mathbf{X}_{.N}^T]^T \in \mathbb{C}^{I_3 N \times M}$ and $\mathbf{X}_3 = [\mathbf{X}_{1..}^T \dots \mathbf{X}_{M..}^T]^T \in \mathbb{C}^{NM \times I_3}$ follows (4) and (5). Comparing (26) and (7) we deduce the following correspondences: $\mathbf{A} \rightarrow \mathbf{A}$, $\mathbf{B} \rightarrow \mathbf{S}^T$ and $\mathbf{C} \rightarrow \mathbf{W}$. The link of the general PARAFAC model (7) to the tensor model of each considered system is provided in Table 1 for comparison.

	Oversampled	DS/CDMA	OFDM
(I_3)	oversampling(P)	spreading(J)	frequency(F)
(R_2)	delay(K)	delay(K)	frequency(F)
W	$\mathbf{H} = [\mathbf{H}^{(1)} \dots \mathbf{H}^{(Q)}]$	$\mathbf{U} = [\mathbf{U}^{(1)} \dots \mathbf{U}^{(Q)}]$	$\mathbf{\Lambda} = [\mathbf{\Lambda}^{(1)} \dots \mathbf{\Lambda}^{(Q)}]$
dimensions	$P \times QLK$	$J \times QLK$	$F \times QLF$
structure	no structure	no structure	diagonal blocks
Matrix S	$\mathbf{S} = [\mathbf{S}^{(1)T} \dots \mathbf{S}^{(Q)T}]^T$	$\mathbf{S} = [\mathbf{S}^{(1)T} \dots \mathbf{S}^{(Q)T}]^T$	$\mathbf{S} = [\mathbf{S}^{(1)T} \dots \mathbf{S}^{(Q)T}]^T$
dimensions	$QK \times N$	$QK \times N$	$QF \times N$
structure	block-Toeplitz	block-Toeplitz	no structure

Table 1. Link of the PARAFAC model for each communication system

6 Application to Blind Multiuser Equalization

The blind multiuser equalization problem consists in recovering the information sequence from several users under the assumption of frequency-selective fading. In other words, a blind multiuser equalizer performs the tasks of signal separation and equalization. In this paper, we propose a PARAFAC-based receiver performing user separation and equalization iteratively. For the temporally-oversampled system, multiuser signal separation is carried out in the 3D tensor space, exploiting *oversampling*, *time* and *space* dimensions of the received signal.

The alternating least squares (ALS) method [6] is used for this purpose. Equalization is done in the 2D matrix space, where the Toeplitz structure of the symbol matrix as well as the Finite-Alphabet (FA) property of the transmitted symbols are exploited to estimate the transmitted symbols via a subspace method. The key aspect of the proposed algorithm is that multiuser signal separation (PARAFAC stage) and equalization (Subspace+FA stage) is done in an iterative way. The goal of the PARAFAC stage is to estimate three

component matrices from which the PARAFAC model parameters can be determined. In turn, the goal of the subspace+FA stage is to solve the partial rotation ambiguity problem that is inherent to the proposed model as well as to estimate the transmitted symbols in the 2D space, exploiting the FA property. The FA-projected symbols are in turn used as an input to the PARAFAC stage to refine the multiuser signal separation in the 3D space. In the following, we describe the proposed algorithm.

6.1 Iterative PARAFAC-Subspace Receiver

For the received signal tensor \mathcal{X} ($M \times N \times P$), multiuser signal separation is carried out in the 3D tensor space using the ALS algorithm, which consists in estimating in an alternating way three matrices $\hat{\mathbf{Z}}_1 \in \mathbb{C}^{N \times KQ}$, $\hat{\mathbf{Z}}_2 \in \mathbb{C}^{M \times LQ}$ and $\hat{\mathbf{Z}}_3 \in \mathbb{C}^{P \times KLQ}$ from the matrix representations $\mathbf{X}_{i=1,2,3}$ of the received signal tensor. The multiuser signal separation problem is formulated as a set of three independent nonlinear least squares problems:

$$\begin{aligned}\hat{\mathbf{Z}}_1 &= \underset{\mathbf{Z}_1}{\operatorname{argmin}} \|\mathbf{X}_1 - (\mathbf{Z}_3 \diamond \mathbf{Z}_2 \bar{\Psi})(\mathbf{Z}_1 \bar{\Phi})^T\|_F^2, \\ \hat{\mathbf{Z}}_2 &= \underset{\mathbf{Z}_2}{\operatorname{argmin}} \|\mathbf{X}_2 - (\mathbf{Z}_1 \bar{\Phi} \diamond \mathbf{Z}_3)(\mathbf{Z}_2 \bar{\Psi})^T\|_F^2, \\ \hat{\mathbf{Z}}_3 &= \underset{\mathbf{Z}_3}{\operatorname{argmin}} \|\mathbf{X}_3 - (\mathbf{Z}_2 \bar{\Psi} \diamond \mathbf{Z}_1 \bar{\Phi})\mathbf{Z}_3^T\|_F^2.\end{aligned}\tag{27}$$

Thus, one iteration of the multiuser signal separation stage has three steps. At each step one component matrix is updated while the others are fixed to the values obtained at the previous step. By analogy with (26), we have $\mathbf{Z}_1 \rightarrow \mathbf{S}$, $\mathbf{Z}_2 \rightarrow \mathbf{A}$ and $\mathbf{Z}_3 \rightarrow \mathbf{W}$. Uniqueness of \mathbf{A} and \mathbf{W} is not important in the present context since we are interested in recovering the user symbol sequences (which is the final goal in the blind multiuser equalization problem) that should be extracted from \mathbf{S} . From (11), and ignoring the trivial permutation ambiguity, we have:

$$\hat{\mathbf{S}}^{(1)} = \mathbf{T}^{(1)}\mathbf{S}^{(1)} \quad , \dots , \quad \hat{\mathbf{S}}^{(Q)} = \mathbf{T}^{(Q)}\mathbf{S}^{(Q)},$$

where $\mathbf{T}^{(q)}$, $q = 1, \dots, Q$ are non-singular (ambiguity) matrices to be determined. The determination of $\mathbf{T}^{(q)}$ and $\hat{\mathbf{S}}^{(q)}$ can be viewed as an equivalent single-input multiple-output (SIMO) blind channel identification problem, where $\mathbf{T}^{(q)}$, $q = 1, \dots, Q$ play the role of virtual length- K SIMO channels with K outputs. The subspace+FA stage of the proposed receiver aims at determining $\mathbf{T}^{(q)}$, $q = 1, \dots, Q$, by the following steps. Matrices $\hat{\mathbf{T}}^{(1)}, \dots, \hat{\mathbf{T}}^{(Q)}$ are determined at each ALS iteration, via a subspace method. In this work we use the subspace method originally proposed by Moulines et al. in [31]. For reasons of space, we report the interested reader to the original work for further details. After determining $\hat{\mathbf{T}}^{(q)}$, the associated symbol matrix $\hat{\mathbf{S}}^{(q)}$

$i = 0$; Initialize $\widehat{\mathbf{Z}}_2(0)$ and $\widehat{\mathbf{Z}}_3(0)$
1. $i = i + 1$;
2. Update $\widehat{\mathbf{Z}}_1^T(i) = [(\widehat{\mathbf{Z}}_3(i-1) \diamond \widehat{\mathbf{Z}}_2(i-1) \overline{\Psi}) \overline{\Phi}^T]^\dagger \mathbf{X}_1$;
3. Subspace+FA stage (go to table 3);
4. Form $\widehat{\mathbf{Z}}_1(i) = [\widehat{\mathbf{Z}}_1^{(1)}(i) \cdots \widehat{\mathbf{Z}}_1^{(Q)}(i)]$;
5. Update $\widehat{\mathbf{Z}}_2^T(i) = [(\widehat{\mathbf{Z}}_1(i) \overline{\Phi} \diamond \widehat{\mathbf{Z}}_3(i-1)) \overline{\Psi}^T]^\dagger \mathbf{X}_2$;
6. Update $\widehat{\mathbf{Z}}_3^T(i) = [\widehat{\mathbf{Z}}_2(i) \Psi \diamond \widehat{\mathbf{Z}}_1(i) \overline{\Phi}]^\dagger \mathbf{X}_3$;
7. Go to step 1 until convergence.

Table 2. Pseudo-code for the iterative PARAFAC-Subspace algorithm

for $q = 1$ to Q ,
– Partition $\widehat{\mathbf{Z}}_1(i) = [\widehat{\mathbf{Z}}_1^{(1)}(i) \cdots \widehat{\mathbf{Z}}_1^{(Q)}(i)]$;
– Determine $\mathbf{T}^{(q)}(i)$ from $\widehat{\mathbf{Z}}_1^{(q)}(i)$ (subspace method);
– $\widehat{\mathbf{S}}^{(q)}(i) = [\widehat{\mathbf{T}}^{(q)}(i)]^{-1} \widehat{\mathbf{Z}}_1^{(q)}(i)$;
– $\widehat{\mathbf{s}}^{(q)}(i) = \text{Average over the columns of } \widehat{\mathbf{S}}^{(q)}(i)$;
– $\widetilde{\mathbf{s}}^{(q)}(i) = \text{Proj}[\widehat{\mathbf{s}}^{(q)}(i)]$;
– $\widehat{\mathbf{Z}}_1^{(q)}(i) = \text{Toeplitz}[\widetilde{\mathbf{s}}^{(q)}(i)]$;
end q

Table 3. Pseudo-code for the subspace + FA projection stage

can be estimated (up to permutation) by pseudo-inversion. An estimation of user symbol sequences $\widehat{\mathbf{s}}^{(q)} \in \mathbb{C}^N$ is obtained by properly averaging over the columns of $\widehat{\mathbf{S}}^{(q)}$ followed by a FA-projection. We assume that the first symbol of each user sequence is known and equal to 1. This allows us to eliminate scaling ambiguity by normalizing each estimated symbol sequence $\widetilde{\mathbf{s}}^{(q)}(i)$ by its first element. An updated (post-equalized) version of $\widehat{\mathbf{Z}}_1$ is then formed and used as an input to the PARAFAC stage to refine user signal separation in the 3D space. At the end of the algorithm, the permutation ambiguity is resolved using a greedy least squares ($\mathbf{S}^{(q)}, \widehat{\mathbf{S}}^{(q)}$)-column matching algorithm [11].

Tables 2 and 3 summarize the proposed iterative PARAFAC-Subspace algorithm. Table 2 describes the steps of the proposed algorithm, with emphasis on the ALS algorithm. In table 3 the steps associated with the subspace+FA stage are detailed. The operator $\text{Proj}[\cdot]$ projects each entry of its vector argument to the closest point of the finite symbol alphabet. At the end of the i -th iteration, an overall error measurement between the estimated model and the

received signal tensor can be obtained from the following equation:

$$e_i = \left\| \mathbf{X}_1 - \left(\hat{\mathbf{Z}}_3(i) \diamond \hat{\mathbf{Z}}_2(i) \overline{\mathbf{\Psi}} \right) \left(\hat{\mathbf{Z}}_1(i) \overline{\mathbf{\Phi}} \right)^T \right\|_F. \quad (28)$$

We declare convergence at the i -th iteration when $|e_i - e_{i-1}| \leq 10^{-5}$.

7 Simulation results

In this section, the performance of the proposed PARAFAC-based blind multiuser receiver is evaluated through computer simulations. Each obtained result is an average over $R = 1000$ independent Monte Carlo runs. For each run, multipath fading gains are generated from an i.i.d. Rayleigh generator while the user symbols are generated from an i.i.d. distribution and are modulated using binary-phase shift keying (BPSK). Perfect synchronization is assumed at the receiver. In all cases, a block of $N = 100$ received samples is used in the blind estimation process. The channel impulse response follows a raised cosine pulse shape with roll-off factor 0.35. We consider $K = 2$ channel taps, $Q = 2$ users and a fixed oversampling factor $P = 8$. At the beginning of the algorithm $\hat{\mathbf{Z}}_2^{(0)}$ and $\hat{\mathbf{Z}}_3^{(0)}$ are randomly initialized. More sophisticated initialization strategies exist, which are based on Tucker3 compression [11] or on eigenanalysis [12], but they are beyond the scope of this work. We have observed however that convergence of the estimates is rapidly achieved (within 10 ALS iterations in most of cases), and this is attributed to the use of the FA property within the ALS loops.

7.1 BER calculation

We adopt the following criterion for the Bit-Error-Rate (BER) calculation. 1% of the total number of runs are discarded, corresponding to inevitable bad runs that reach a local minimum. The criterion for selecting the bad runs is based on the observation of the steady state estimation error, i.e., the error between the received tensor and the tensor constructed from estimated components matrices after convergence. The runs with the highest non-convergent error values are discarded from the BER averaging process. For the bit-error-rate (BER) *versus* signal-to-noise ratio (SNR) results, the BER shown is the BER averaged over both users and R independent runs, i.e.:

$$\text{BER} = \frac{1}{R} \sum_{r=1}^R \frac{\text{BER}_1(r) + \text{BER}_2(r)}{2},$$

where $\text{BER}_1(r)$ and $\text{BER}_2(r)$ is the BER of the first and second users at the r -th run, respectively.

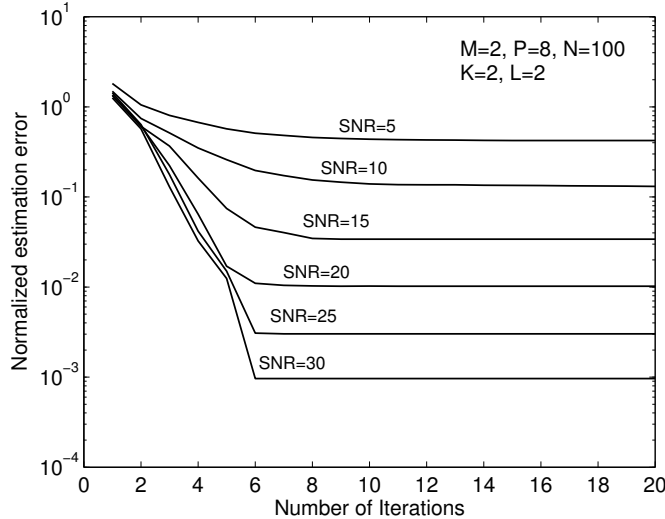


Fig. 4. Convergence of the PARAFAC-Subspace receiver. First propagation scenario.

7.2 Propagation scenarios

We adopt the multipath propagation model described in Section 3 and consider $L = 2$ effective multipaths per user, each path being associated with a different cluster of scatterers. Cluster angle spreads are the same for both users and are given by $(\Delta\theta_{1q}, \Delta\theta_{2q}) = (0^\circ, 5^\circ)$, $q = 1, 2$. Concerning the mean angle of arrival, we consider two propagation scenarios. In the first one, we have $(\theta_{11}, \theta_{21}) = (0^\circ, 20^\circ)$ for the first user and $(\theta_{12}, \theta_{22}) = (-10^\circ, 10^\circ)$ for the second one. The second propagation scenario is more challenging. The mean angle of arrival of the first (zero-delayed) path of both users is identical, and we have $\theta_{11} = \theta_{12} = 0^\circ$, while the other multipaths have the same angles as those of the first scenario. Unless otherwise stated, all multipaths have the same average power $E[\beta_{lq}\beta_{lq}^*] = 1$, $l = 1, \dots, L$, $q = 1, \dots, Q$.

7.3 Performance results

We begin by evaluating the convergence of the proposed PARAFAC-Subspace algorithm. Figure 4 shows typical convergence curves, considering the first propagation scenario. The median values of the normalized error $e_i^2/(MPN)$, where e_i is given in 28, are plotted as a function of the iterations for various SNR values. It can be seen from Fig. 4 that the algorithm rapidly converges, usually within 10 iterations. We have observed that convergence is actually accelerated due to the use of FA property within the ALS loops.

Now, BER versus SNR results are evaluated considering the first scenario, where users have distinct spatial signatures. In order to verify the influence of

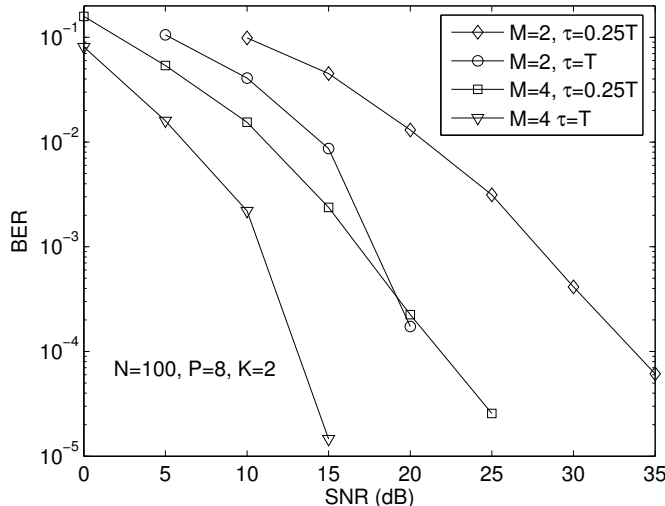


Fig. 5. BER versus SNR results. First propagation scenario.

the multipath delay spread, we consider two cases. In the first one $(\tau_{1q}, \tau_{2q}) = (0, \tau) = (0, T)$, while in the second one $(\tau_{1q}, \tau_{2q}) = (0, \tau) = (0, 0.25T)$, $q = 1, 2$. The results are shown in Figure 5, for $M = 2$ and 4 receive antennas. It can be seen that the BER performance of the proposed receiver is remarkable, even with $M = 2$ receive antennas. A significant performance gain is observed when the number of receive antennas is increased from 2 to 4, since more degrees of freedom are available in the space domain to separate the two user signals. Improved performance is obtained when $\tau = T$, i.e., when the delay of the second multipath (for both users) coincides with one symbol period. Multipath combination is more effective when $\tau = T$, since the multipaths are better distinguished in the time domain. Moreover, when $\tau = 0.25T$, some multipath energy is spread beyond $K = 2$ symbol periods and this is ignored in our tensor model.

We now consider the second propagation scenario, where the first path of both users have identical angles of arrival. We want to illustrate that in this type of scenario, path diversity becomes important and frequency-selectivity indeed helps the separability of the user signals in the time domain. In order to evaluate this, the average power of the second (one-symbol delayed) path of each user is varied. We define δ as the average ratio between the gain of the second and first multipaths, which are assumed equal for both users. We consider $\delta = 0.1, 0.25, 0.5$ and 1. According to Figure 6, improved performance is obtained when the first and second paths have the same average power, i.e., $\delta = 1$. In this case, the path diversity gain is maximum. The worst result is obtained with $\delta = 0.1$ (nearly flat-fading channel). These results indicate that the proposed PARAFAC-Subspace receiver effectively combines the multipaths of each user to provide a path diversity gain, being able to blindly separate the two user signals.

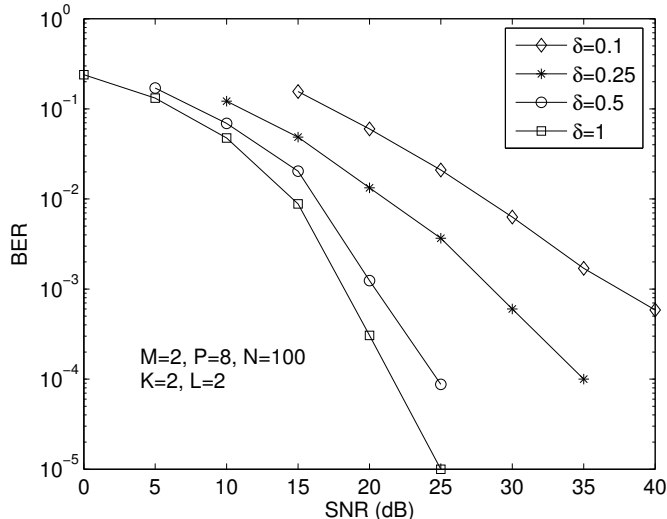


Fig. 6. BER versus SNR results. Second propagation scenario.

In order to provide a performance reference for the proposed PARAFAC-Subspace receiver, we also evaluate the performance of the Minimum Mean Square Error (MMSE) receiver. In contrast to our blind iterative PARAFAC-Subspace receiver, the MMSE one assumes perfect knowledge of all channel parameters as well as the knowledge of the SNR. We consider $M = 2$ and 4 receive antennas. Figure 7 shows that the PARAFAC-Subspace receiver has nearly the same BER vs. SNR improvement than that of MMSE with perfect channel knowledge. The gap between both receivers is smaller for $M = 4$. For example, considering a target BER of 10^{-2} , the proposed receiver provides a loss in performance of 5dB for $M = 2$ and 3dB for $M = 4$, with respect to the MMSE receiver.

8 Conclusions and Perspectives

In this paper, we have proposed a unified PARAFAC-based modeling approach for the received signal of three multiuser wireless communication systems employing an antenna array and subject to frequency-selective multipath propagation: Temporally-oversampled, DS/CDMA and OFDM systems. It turned out that the proposed 3D PARAFAC model is subject to structural constraints within two of its component matrices, associated with the space and time dimensions of the received signal tensor. The interesting aspect of the proposed modeling approach is that the same “general” PARAFAC model is shared by the three considered systems and the model for each particular system can be derived from the general model by making appropriate choices for the structure and/or dimensions of its component matrices. A new receiver algorithm has been presented as an application of the proposed tensor model for

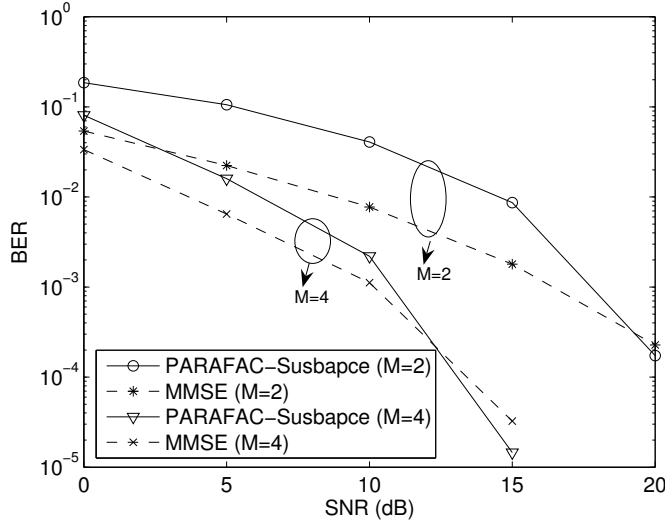


Fig. 7. Blind PARAFAC-Subspace receiver versus MMSE receiver with perfect channel knowledge.

blind multiuser equalization. The proposed algorithm combines PARAFAC and a subspace method together with the use of the FA property in order to perform user signal separation and equalization iteratively. According to our simulation results, the performance of the iterative PARAFAC-Subspace is remarkable and not so far from the MMSE solution with perfect knowledge of propagation parameters.

Perspectives of this work are multi-fold. From a theoretical point of view, the impact of use of the FA property on the identifiability conditions of the proposed tensor model is an open question and deserves more study. One can expect that the use of the FA property leads to more relaxed identifiability conditions. We have observed that experimentally, but we have not yet proved this analytically. The exploitation of the Constant Modulus (CM) property in addition to the FA property in the context of the proposed tensor model is also an open topic. A recent work [21] has provided a link between the identifiability of PARAFAC and CM factorizations. Therefore, it may be useful to study the identifiability of the proposed model subject to FA/CM constraints, following the approach of [21]. The Vandermonde structure of the matrix of spatial responses \mathbf{A} could also be exploited. Finally, the application of the proposed receiver algorithm to the blind signal separation of DS/CDMA and OFDM signals is also a research topic for further work.

Appendix

Here, we provide a demonstration of (7). This is done by expanding the tensor x_{i_1, i_2, i_3} in (6) using Kronecker products of canonical vectors [32]:

$$x_{i_1, i_2, i_3} = \sum_{q=1}^Q \sum_{r_1=1}^{R_1} \sum_{r_2=1}^{R_2} a_{i_1, r_1}^{(q)} b_{i_2, r_2}^{(q)} c_{r_1, r_2, i_3}^{(q)}. \quad (29)$$

Consider the canonical bases $\mathbf{E}^{(I_1)} = \{\mathbf{e}_1^{(I_1)}, \mathbf{e}_2^{(I_1)}, \dots, \mathbf{e}_{I_1}^{(I_1)}\}$, $\mathbf{E}^{(I_2)} = \{\mathbf{e}_1^{(I_2)}, \mathbf{e}_2^{(I_2)}, \dots, \mathbf{e}_{I_2}^{(I_2)}\}$ and $\mathbf{E}^{(I_3)} = \{\mathbf{e}_1^{(I_3)}, \mathbf{e}_2^{(I_3)}, \dots, \mathbf{e}_{I_3}^{(I_3)}\}$ associated with vector spaces \mathbb{R}^{I_1} , \mathbb{R}^{I_2} , \mathbb{R}^{I_3} , respectively. The unfolded matrix $\mathbf{X}_3 \in \mathbb{C}^{I_1 I_2 \times I_3}$, defined as $x_{i_1, i_2, i_3} = [\mathbf{X}_3]_{(i_1-1)I_2 + i_2, i_3}$, can be expanded in terms of these canonical vectors in the following manner:

$$\mathbf{X}_3 = \sum_{i_1=1}^{I_1} \sum_{i_2=1}^{I_2} \sum_{i_3=1}^{I_3} x_{i_1, i_2, i_3} (\mathbf{e}_{i_1}^{(I_1)} \otimes \mathbf{e}_{i_2}^{(I_2)}) \mathbf{e}_{i_3}^{(I_3)T}. \quad (30)$$

Substituting (29) into (30) we have:

$$\begin{aligned} \mathbf{X}_3 &= \sum_{i_1=1}^{I_1} \sum_{i_2=1}^{I_2} \sum_{i_3=1}^{I_3} \sum_{q=1}^Q \sum_{r_1=1}^{R_1} \sum_{r_2=1}^{R_2} a_{i_1, r_1}^{(q)} b_{i_2, r_2}^{(q)} c_{r_1, r_2, i_3}^{(q)} (\mathbf{e}_{i_1}^{(I_1)} \otimes \mathbf{e}_{i_2}^{(I_2)}) \mathbf{e}_{i_3}^{(I_3)T} \\ &= \sum_{q=1}^Q \sum_{r_1=1}^{R_1} \sum_{r_2=1}^{R_2} \left(\sum_{i_1=1}^{I_1} \mathbf{e}_{i_1}^{(I_1)} a_{i_1, r_1}^{(q)} \right) \otimes \left(\sum_{i_2=1}^{I_2} \mathbf{e}_{i_2}^{(I_2)} b_{i_2, r_2}^{(q)} \right) \left(\sum_{i_3=1}^{I_3} \mathbf{e}_{i_3}^{(I_3)} c_{r_1, r_2, i_3}^{(q)} \right)^T. \end{aligned}$$

Define $\mathbf{a}_{r_1}^{(q)}$ as the r_1 -th column of $\mathbf{A}^{(q)} \in \mathbb{C}^{I_1 \times R_1}$, $\mathbf{b}_{r_2}^{(q)}$ as the r_2 -th column of $\mathbf{B}^{(q)} \in \mathbb{C}^{I_2 \times R_2}$ and $\mathbf{c}_{r_1, r_2}^{(q)}$ as the $[(r_1 - 1)R_2 + r_2]$ -th column of $\mathbf{C}^{(q)} \in \mathbb{C}^{I_3 \times R_1 R_2}$, and observe that:

$$\sum_{i_1=1}^{I_1} \mathbf{e}_{i_1}^{(I_1)} a_{i_1, r_1}^{(q)} = \mathbf{a}_{r_1}^{(q)}, \quad \sum_{i_2=1}^{I_2} \mathbf{e}_{i_2}^{(I_2)} b_{i_2, r_2}^{(q)} = \mathbf{b}_{r_2}^{(q)}, \quad \sum_{i_3=1}^{I_3} \mathbf{e}_{i_3}^{(I_3)} c_{r_1, r_2, i_3}^{(q)} = \mathbf{c}_{r_1, r_2}^{(q)},$$

we have:

$$\mathbf{X}_3 = \sum_{q=1}^Q \sum_{r_1=1}^{R_1} \sum_{r_2=1}^{R_2} (\mathbf{a}_{r_1}^{(q)} \otimes \mathbf{b}_{r_2}^{(q)}) \mathbf{c}_{r_1, r_2}^{(q)T}. \quad (31)$$

Define the set of canonical vectors $\mathbf{e}_{r_2}^{(R_2)}$, $r_2 = 1, \dots, R_2$. Inserting $(\mathbf{e}_{r_2}^{(R_2)})^T \mathbf{e}_{r_2}^{(R_2)} = 1$ into (31) gives:

$$\mathbf{X}_3 = \sum_{q=1}^Q \sum_{r_1=1}^{R_1} \sum_{r_2=1}^{R_2} [(\mathbf{a}_{r_1}^{(q)} \otimes \mathbf{b}_{r_2}^{(q)}) \mathbf{e}_{r_2}^{(R_2)T}] [\mathbf{e}_{r_2}^{(R_2)} \mathbf{c}_{r_1, r_2}^{(q)T}]. \quad (32)$$

Considering the following property:

$$(\mathbf{a} \otimes \mathbf{b}) \mathbf{c}^T = \mathbf{a} \mathbf{1}_{n_c}^T \diamond \mathbf{b} \mathbf{c}^T,$$

with $\mathbf{a} \in \mathbb{C}^{n_a}$, $\mathbf{b} \in \mathbb{C}^{n_b}$, $\mathbf{c} \in \mathbb{C}^{n_c}$ and $\mathbf{1}_{n_c} \in \mathbb{C}^{n_c}$, we can rewrite (32) as:

$$\begin{aligned} \mathbf{X}_3 &= \sum_{q=1}^Q \sum_{r_1=1}^{R_1} \sum_{r_2=1}^{R_2} \left[\mathbf{a}_{r_1}^{(q)} \mathbf{1}_{R_2}^T \diamond \mathbf{b}_{r_2}^{(q)} \mathbf{e}_{r_2}^{(R_2)T} \right] \left[\mathbf{e}_{r_2}^{(R_2)} \mathbf{c}_{r_1, r_2}^{(q)T} \right] \\ &= \sum_{q=1}^Q \sum_{r_1=1}^{R_1} \sum_{r_2=1}^{R_2} \left[\sum_{i=1}^{R_2} \left(\mathbf{a}_{r_1}^{(q)} \mathbf{e}_i^{(R_2)T} \diamond \mathbf{b}_{r_2}^{(q)} \mathbf{e}_{r_2}^{(R_2)T} \right) \right] \left[\mathbf{e}_{r_2}^{(R_2)} \mathbf{c}_{r_1, r_2}^{(q)T} \right]. \end{aligned} \quad (33)$$

Since the summation over $i = 1, \dots, R_2$ in brackets is null for every $i \neq r_2$, we can rewrite (33) as:

$$\mathbf{X}_3 = \sum_{q=1}^Q \sum_{r_1=1}^{R_1} \sum_{r_2=1}^{R_2} \left[\mathbf{a}_{r_1}^{(q)} \mathbf{e}_{r_2}^{(R_2)T} \diamond \mathbf{b}_{r_2}^{(q)} \mathbf{e}_{r_2}^{(R_2)T} \right] \left[\mathbf{e}_{r_2}^{(R_2)} \mathbf{c}_{r_1, r_2}^{(q)T} \right]. \quad (34)$$

Due to the presence of the unit vector $\mathbf{e}_{r_2}^{(R_2)}$, we can rewrite (34) as:

$$\begin{aligned} \mathbf{X}_3 &= \sum_{q=1}^Q \sum_{r_1=1}^{R_1} \left[\sum_{r_2=1}^{R_2} \mathbf{a}_{r_1}^{(q)} \mathbf{e}_{r_2}^{(R_2)T} \diamond \sum_{r_2=1}^{R_2} \mathbf{b}_{r_2}^{(q)} \mathbf{e}_{r_2}^{(R_2)T} \right] \left[\sum_{r_2=1}^{R_2} \mathbf{e}_{r_2}^{(R_2)} \mathbf{c}_{r_1, r_2}^{(q)T} \right] \\ &= \sum_{q=1}^Q \sum_{r_1=1}^{R_1} \left[(\mathbf{a}_{r_1}^{(q)} \otimes \mathbf{1}_{R_2}^T) \diamond \mathbf{B}^{(q)} \right] \mathbf{C}_{r_1}^{(q)T}, \end{aligned} \quad (35)$$

with $\mathbf{C}_{r_1}^{(q)} = \sum_{r_2=1}^{R_2} \mathbf{c}_{r_1, r_2}^{(q)} \mathbf{e}_{r_2}^{(R_2)T} \in \mathbb{C}^{I_3 \times R_2}$.

Now, consider the set of canonical vectors $\mathbf{e}_{r_1}^{(R_1)}$, $r_1 = 1, \dots, R_1$. Inserting $\mathbf{e}_{r_1}^{(R_1)T} \mathbf{e}_{r_1}^{(R_1)} = 1$ into (35) and using property (1), it follows that:

$$\begin{aligned} \mathbf{X}_3 &= \sum_{q=1}^Q \sum_{r_1=1}^{R_1} \mathbf{e}_{r_1}^{(R_1)T} \mathbf{e}_{r_1}^{(R_1)} \otimes \left[(\mathbf{a}_{r_1}^{(q)} \otimes \mathbf{1}_{R_2}^T) \diamond \mathbf{B}^{(q)} \right] \mathbf{C}_{r_1}^{(q)T} \\ &= \sum_{q=1}^Q \sum_{r_1=1}^{R_1} \left[\mathbf{e}_{r_1}^{(R_1)T} \otimes \left[(\mathbf{a}_{r_1}^{(q)} \otimes \mathbf{1}_{R_2}^T) \diamond \mathbf{B}^{(q)} \right] \right] \cdot \left[\mathbf{e}_{r_1}^{(R_1)} \otimes \mathbf{C}_{r_1}^{(q)T} \right]. \end{aligned} \quad (36)$$

Note that:

$$\mathbf{e}_{r_1}^{(R_1)T} \otimes \left[(\mathbf{a}_{r_1}^{(q)} \otimes \mathbf{1}_{R_2}^T) \diamond \mathbf{B}^{(q)} \right] = \left[\mathbf{e}_{r_1}^{(R_1)T} \otimes (\mathbf{a}_{r_1}^{(q)} \otimes \mathbf{1}_{R_2}^T) \right] \diamond \left[\mathbf{e}_{r_1}^{(R_1)T} \otimes \mathbf{B}^{(q)} \right],$$

which allows us to express (36) in the following form:

$$\mathbf{X}_3 = \sum_{q=1}^Q \sum_{r_1=1}^{R_1} \left[\left[\mathbf{e}_{r_1}^{(R_1)T} \otimes (\mathbf{a}_{r_1}^{(q)} \otimes \mathbf{1}_{R_2}^T) \right] \diamond \left[\mathbf{e}_{r_1}^{(R_1)T} \otimes \mathbf{B}^{(q)} \right] \right] \cdot \left[\mathbf{e}_{r_1}^{(R_1)} \otimes \mathbf{C}_{r_1}^{(q)T} \right]. \quad (37)$$

Due to the block structure with zeros introduced by the factor $\mathbf{e}_{r_1}^{(R_1)}$, we can rewrite (37) as:

$$\mathbf{X}_3 = \sum_{q=1}^Q \left\{ \left[\sum_{r_1=1}^{R_1} \mathbf{e}_{r_1}^{(R_1)T} \otimes (\mathbf{a}_{r_1}^{(q)} \otimes \mathbf{1}_{R_2}^T) \right] \diamond \left[\sum_{r_1=1}^{R_1} \mathbf{e}_{r_1}^{(R_1)T} \otimes \mathbf{B}^{(q)} \right] \right\} \cdot \left[\sum_{r_1=1}^{R_1} \mathbf{e}_{r_1}^{(R_1)} \otimes \mathbf{C}_{r_1}^{(q)T} \right] \quad (38)$$

which leads to:

$$\mathbf{X}_3 = \sum_{q=1}^Q \left[(\mathbf{A}^{(q)} \otimes \mathbf{1}_{R_2}^T) \diamond (\mathbf{1}_{R_1}^T \otimes \mathbf{B}^{(q)}) \right] \cdot \mathbf{C}^{(q)T}. \quad (39)$$

Now, using the property (1) of the Kronecker product, we have:

$$\mathbf{A}^{(q)} \otimes \mathbf{1}_{R_2}^T = (\mathbf{A}^{(q)} \otimes \mathbf{1})(\mathbf{I}_{R_1} \otimes \mathbf{1}_{R_2}^T) = \mathbf{A}^{(q)} \underbrace{(\mathbf{I}_{R_1} \otimes \mathbf{1}_{R_2}^T)}_{\Psi} = \mathbf{A}^{(q)} \Psi,$$

and

$$\mathbf{1}_{R_1}^T \otimes \mathbf{B}^{(q)} = (\mathbf{1} \otimes \mathbf{B}^{(q)})(\mathbf{1}_{R_1}^T \otimes \mathbf{I}_{R_2}) = \mathbf{B}^{(q)} \underbrace{(\mathbf{1}_{R_1}^T \otimes \mathbf{I}_{R_2})}_{\Phi} = \mathbf{B}^{(q)} \Phi,$$

and (39) can be expressed as:

$$\mathbf{X}_3 = \sum_{q=1}^Q (\mathbf{A}^{(q)} \Psi \diamond \mathbf{B}^{(q)} \Phi) \mathbf{C}^{(q)T}. \quad (40)$$

Defining $\mathbf{A} = [\mathbf{A}^{(1)} \dots \mathbf{A}^{(Q)}] \in \mathbb{C}^{I_1 \times QR_1}$, $\mathbf{B} = [\mathbf{B}^{(1)} \dots \mathbf{B}^{(Q)}] \in \mathbb{C}^{I_2 \times QR_2}$ and $\mathbf{C} = [\mathbf{C}^{(1)} \dots \mathbf{C}^{(Q)}] \in \mathbb{C}^{I_3 \times QR_1 R_2}$, and $\bar{\Psi} = \mathbf{I}_Q \otimes \Psi$ and $\bar{\Phi} = \mathbf{I}_Q \otimes \Phi$, we can equivalently write (40) as:

$$\mathbf{X}_3 = (\mathbf{A} \bar{\Psi} \diamond \mathbf{B} \bar{\Phi}) \mathbf{C}^T,$$

and the demonstration of (7) is finished.

References

- [1] A. J. Paulraj, C. B. Papadias, "Space-time processing for wireless communications," *IEEE Sig. Proc. Mag.*, vol. 14, pp. 49–83, 1997.
- [2] S. Talwar, M. Viberg, A. J. Paulraj, "Blind separation of synchronous co-channel digital signals using an antenna array—Part I: Algorithms," *IEEE Trans. on Sig. Proc.*, vol. 44, pp. 1184–1197, 1996.
- [3] A. -J. van der Veen, "A subspace approach for blind space-time signal processing," *IEEE Trans. on Sig. Proc.*, vol. 45, no. 1, pp. 173–190, 1997.

- [4] J. B. Kruskal, "Three-way arrays: Rank and uniqueness of trilinear decompositions with applications to arithmetic complexity and statistics," *Linear Algebra Applicat.*, vol. 18, pp. 95–138, 1977.
- [5] J. D. Carroll, J. Chang, "Analysis of individual differences in multidimensional scaling via an n -way generalization of "Eckart-Young" decomposition," *Psychometrika*, vol. 35, no. 3, pp. 283–319, 1970.
- [6] R. A. Harshman, "Foundations of the PARAFAC procedure: Model and conditions for an "explanatory" multi-mode factor analysis," *UCLA Working papers in phonetics*, vol. 16, no. 1, pp. 1–84, 1970.
- [7] R. Bro, Multi-way analysis in the food industry: models, algorithms and applications, Ph.D. thesis, University of Amsterdam (NL), 1998.
- [8] N. D. Sidiropoulos, "Low-rank decomposition of multi-way arrays: A signal processing perspective," *SAM 2004*, Barcelona, Spain, July 2004.
- [9] N. D. Sidiropoulos, G. B. Giannakis, R. Bro, "Parallel factor analysis in sensor array processing," *IEEE Trans. on Sig. Proc.*, vol. 48, no. 8, pp. 2377–2388, 2000.
- [10] R. Roy, T. Kailath, "ESPRIT—Estimation of signal parameters via rotational invariance techniques," *IEEE Trans. on Acoustics Speech and Sig. Proc.*, vol. 37, pp. 984–995, 1989.
- [11] N. D. Sidiropoulos, R. Bro, G. B. Giannakis, "Blind PARAFAC receivers for DS/CDMA systems," *IEEE Trans. on Sig. Proc.*, vol. 48, no. 3, pp. 810–823, 2000.
- [12] N. D. Sidiropoulos, G. Z. Dimic, "Blind multiuser detection in WCDMA systems with large delay spread," *IEEE Signal Processing Letters*, vol. 8, no. 3, pp. 87–89, 2001.
- [13] A. de Baynast and L. De Lathauwer, "Détection autodidacte pour des systèmes à accès multiple basée sur l'analyse PARAFAC," *Proc. of XIX GRETSI Symp. Sig. Image Proc.*, Paris, France, September 2003.
- [14] A. de Baynast, L. De Lathauwer, B. Aazhang, "Blind PARAFAC receivers for multiple access-multiple antenna systems," in *Proc. of VTC Fall 2003*, Orlando, USA, October 2003.
- [15] T. Jiang, N. D. Sidiropoulos, "A direct semi-blind receiver for SIMO and MIMO OFDM systems subject to frequency offset," in *Proc. of SPAWC 2003*, Rome, Italy, June 2003.
- [16] J. G. Proakis, *Digital Communications*, 4th Edition, McGraw-Hill, New York, 2001.
- [17] R. D. van Nee, R. Prasad, *OFDM for wireless multimedia communications*, 1st Edition, Artech House, 2000.

- [18] N. D. Sidiropoulos and X. Liu, "Identifiability results for blind beamforming in incoherent multipath with small delay spread," *IEEE Trans. Sig. Proc.*, vol. 49, n. 1, pp.228–236, January 2001.
- [19] R. A. Harshman, "Determination and proof of minimum uniqueness conditions for PARAFAC1, *UCLA Working Papers in Phonetics*, n. 22, pp. 111–117, 1972.
- [20] J. M. F. ten Berge, N. D. Sidiropoulos, "On uniqueness in CANDECOMP/PARAFAC," *Psychometrika*, vol. 67, pp. 399–409, 2002.
- [21] T. Jiang, N. D. Sidiropoulos, "Kruskal's permutation lemma and the identification of CANDECOMP/PARAFAC and bilinear models with constant modulus constraints," *IEEE Trans. on Sig. Proc.*, vol. 52, n. 9, pp. 2625–2636, 2004.
- [22] N. D. Sidiropoulos, R. Bro, "On the uniqueness of multilinear decomposition of N-way arrays," *Journal of Chemometrics*, vol. 14, pp. 229–239, 2000.
- [23] X. Liu, N. D. Sidiropoulos, "Cramer-Rao bounds for low-rank decomposition of multidimensional arrays," *IEEE Trans. on Sig. Proc.*, vol. 49, no. 9, pp. 2074–2086, 2001.
- [24] D. Astély, "On Antenna Arrays in Mobile Communication Systems: Fast Fading and GSM Base Station Receiver Algorithms," Royal Institute of Technology, Stockholm, Sweden, IR-S3-SB-9611, 1996.
- [25] J. Fuhl, A. F. Molisch, E. Bonek, "Unified channel model for mobile radio systems with smart antennas," in *Proc. Inst. Elect. Eng.*, vol. 145, pp. 32-41, Feb. 1998.
- [26] H. Bolcskei, Fuhl, D. Gesbert, A. J. Paulraj, "On the Capacity of OFDM-Based Spatial Multiplexing Systems," *IEEE Trans. on Commun.*, vol. 50, n. 2, pp. 225–234, Feb. 2002.
- [27] R. B. Ertel, P. Cardieri, K. W. Sowerby, T. S. Rappaport, J. H. Reed, "Overview of spatial channel models for antenna array communication systems," *IEEE Personal Commun.*, vol. 5, n. 1, pp. 10-22, Feb. 1998.
- [28] R. Bro, R. A. Harshman, N. D. Sidiropoulos, "Modeling Multi-way data with linearly dependent loadings," *technical report*, KVL, Copenhagen, Denmark, 2005.
- [29] A. L. F. de Almeida, G. Favier, and J. C. M. Mota, "Generalized PARAFAC model for multidimensional wireless communications with application to blind multiuser equalization," in *Proc. 39th ASILOMAR Conf. on Sig. Syst. and Comp.*, Pacific Grove, California, 2005.
- [30] A. L. F. de Almeida, G. Favier, and J. C. M. Mota, "Tensor Models for Deterministic Blind Beamforming: A New Approach based on Block-Tensor Decompositions," European Signal Processing Conference (EUSIPCO), Florence, Italy, 2006, *submitted*.

- [31] E. Moulines, P. Duhamel, J.-F. Cardoso, S. Mayrargue, “Subspace methods for blind identification of multichannel FIR filters,” *IEEE Trans. on Sig. Proc.*, vol. 43, no. 2, pp. 516–525, 1995.
- [32] G. Favier, *Calcul matriciel et tensoriel avec applications à l’automatique et au traitement du signal*, under preparation, 2005.